Review

Designing High-Power-Density Electric Motors for Electric Vehicles with Advanced Magnetic Materials

Youguang Guo [1], Lin Liu [1,*], Xin Ba [1,*], Haiyan Lu [1], Gang Lei [1], Wenliang Yin [2] and Jianguo Zhu [2]

1 Faculty of Engineering and Information Technology, University of Technology Sydney, Ultimo, NSW 2007, Australia; youguang.guo-1@uts.edu.au (Y.G.); haiyan.lu@uts.edu.au (H.L.); gang.lei@uts.edu.au (G.L.)
2 School of Electrical and Information Engineering, The University of Sydney, Camperdown, NSW 2006, Australia; wenliang.yin@sydney.edu.au (W.Y.); jianguo.zhu@sydney.edu.au (J.Z.)
* Correspondence: lin.liu@student.uts.edu.au (L.L.); xin.ba@student.uts.edu.au (X.B.)

Abstract: As we face issues of fossil fuel depletion and environmental pollution, it is becoming increasingly important to transition towards clean renewable energies and electric vehicles (EVs). However, designing electric motors with high power density for EVs can be challenging due to space and weight constraints, as well as issues related to power loss and temperature rise. In order to overcome these challenges, a significant amount of research has been conducted on designing high-power-density electric motors with advanced materials, improved physical and mathematical modeling of materials and the motor system, and system-level multidisciplinary optimization of the entire drive system. These technologies aim to achieve high reliability and optimal performance at the system level. This paper provides an overview of the key technologies for designing high-power-density electric motors for EVs with high reliability and system-level optimal performance, with the focus on advanced magnetic materials and the proper modeling of core losses under two-dimensional or three-dimensional vectorial magnetizations. This paper will also discuss the major challenges associated with designing these motors and the possible future research directions in the field.

Keywords: electric motor analysis; electric motor design; electric vehicle; high-power density electric motor; power loss; advanced magnetic material; material property modeling; system-level design; multi-disciplinary optimization

1. Introduction

1.1. State-of-the-Art

The depletion of fossil fuels and environmental pollution have become critical and pressing problems faced by humanity. To address these issues, significant research efforts have been devoted to the development of clean, renewable energy-based electricity generating systems, particularly wind energy [1–3] and solar photovoltaic (PV) generating plants [4,5]. As a result, most future appliances are expected to be powered by electricity generated from renewable resources rather than fossil fuels. One example is the electrification of transportation, which has attracted considerable interest in research and application [6–10]. Various types of electric transportation vehicles have been developed, ranging from low power electric bikes [11–13], cars [14–18], and buses [19,20] to high-power electric trains [21–23], ships [24–26], and aircraft [27–30]. To drive these electrified vehicles, different types of electric motors have been designed and applied, including induction motors [31–33], switched reluctance motors (SRMs) [34–38], permanent magnet synchronous motors (PMSMs) [39–44], and brushless DC motors [45,46].

In an electric vehicle (EV), space and weight limitations often restrict the size of the electric motor drives. Thus, designing motors with high power density is highly desirable [47–56]. One approach is to increase the operational speed since the motor power is proportional to the speed. However, increasing the operational speed can significantly

increase the motor power loss, leading to high temperature rise and compromising the motor performance and reliability. Therefore, it is crucial to carefully design the motor with low power loss, which implies operational cost savings, environmental friendliness, and appropriate thermal dissipation. Other issues related to high-speed operation, such as mechanical strength and vibration, should also be considered.

Design optimization of high-speed electric motors for electric vehicles is therefore a multi-objective and multi-disciplinary task that has received significant attention in the past few decades. For instance, Eberleh and Hartkopf [47] reported a high-speed induction motor coupled with a two-speed transmission for electric vehicles in 2006. The use of a liquid cooling system increased the continuous output power while reducing the motor size, weight, and costs. In 2007, Huang et al. [48] designed a high-speed claw pole motor using soft magnetic composite material as the stator for low core loss and low manufacturing cost. They considered the rotational core loss and further analyzed the temperature distribution by using thermal networks and three-dimensional finite element analysis with the distributed core loss in 2009 [49]. In 2010, Hosseini et al. [50] analyzed linear synchronous motors for high-speed maglev vehicles, accurately calculating major parameters such as magnetic field distribution and thrust force by solving the Maxwell equations in motor layers using analytical methods.

More recently, Damiano et al. [51] presented the design of a high-speed brushless DC motor with ferrite magnets for electric vehicles in 2017. The developed electromagnetic and mechanical models can consider mutual influence when determining the electric motor geometry. Dang et al. [52] reported the design optimization of a high-speed permanent magnet synchronous motor with flux weakening for electric vehicle applications in the same year. They found a solution to determine the motor size from a given driving cycle. Credo et al. [53] presented the design of high-speed synchronous reluctance motors (Syn-RMs) adopting topology optimization for electric vehicles in 2020. Prakht et al. [54] presented the optimization design of a novel three-phase flux reversal motor composed of three single-phase motors sharing a common shaft in 2021. The torque ripple was reduced, and the motor performance was improved. In 2022, Cui et al. [55] proposed a hybrid rotor structure with additional ferrite magnets in the *d*- and *q*-axis magnetic flux paths, along with rotor surface slotting and GA optimization. The innovative design effectively addresses the issue of excessive eddy current loss in FSCW-PMSMs at high speeds, while also providing a cost-effective solution for EV IPMSMs by reducing the usage of expensive Nd-Fe-B magnets. Mashrouteh et al. [56] designed a multi-actuation model predictive controller that integrates optimal corner torque allocation and active aerodynamics control to enhance the stability of performance vehicles during high-speed maneuvers, considering nonlinear tire behavior and actuator dynamics. In 2023, Credo et al. [57] demonstrated how the Syn-RM is effectively evaluated and optimized for EV applications, considering acceleration time, maximum speed, and flux weakening capabilities. The results show that, despite the motor's limitations, it is possible to meet the requirements through advanced design procedures, as confirmed by experimental tests on a scaled prototype for a city car.

1.2. Motivation

Design optimization of high-power-density electric motors for EVs is a complex and multifaceted challenge that requires careful consideration of multiple factors such as power loss reduction, proper thermal dissipation such as forced cooling design, mechanical component improvements such as bearing, advanced manufacturing technologies, and appropriate types of electric motors such as PMSMs, Syn-RMs, SRMs and axial-flux motors. To tackle these challenges, numerous research efforts have been made in the past few decades [33–57]. This paper aims to provide an overview of the latest advanced technologies used in electric motor design and optimization for high-speed and high-power-density motors used in EVs. Specifically, the focus will be on advanced magnetic materials and their characterization, such as modeling core losses under 2D and 3D vectorial magnetizations.

1.3. Paper Organization

The paper is structured as follows. Section 2 provides an overview of advanced electromagnetic materials and their applications in EV motors. Section 3 discusses the development of modern analysis methods for magnetic properties of electromagnetic materials and their application in motor design and analysis. In Section 4, we briefly summarize the advanced design and optimization techniques, with a focus on the multi-level, multi-objective, multi-disciplinary (MMM), and robust optimization approach to achieve optimal performance of electric motor drive systems. Lastly, Section 5 explores current research trends and major challenges in the field.

2. Application of Advanced Electromagnetic Materials in EV Motors

Achieving higher power density in electric motors typically involves increasing operational speed within the constraints of application and mechanical strength, increasing air gap magnetic flux density within the constraints of core materials, and increasing current density in windings within the constraints of thermal dissipation. As a result, researchers have been focused on developing advanced novel materials that possess improved mechanical, electromagnetic, and thermal properties. By incorporating these materials into the electric motor design, it is possible to further increase power density and improve overall performance [58–104].

2.1. Soft Magnetic Materials

Soft ferromagnetic materials are extensively used as the core components of electrical machines, and their magnetic properties have a direct impact on the machine's overall performance. These properties, including the relationship between magnetic field strength and magnetic flux density, as well as the associated core loss, play a crucial role in determining the efficiency and effectiveness of the machine. In order to enhance the magnetic properties of soft ferromagnetic materials, considerable efforts have been invested in improving various aspects, such as increasing their magnetic permeability, saturation flux density, and reducing specific power loss. These improvements are essential for enhancing the overall efficiency and performance of electrical machines. To achieve these goals, researchers and engineers have developed various techniques, such as optimizing material composition and microstructure, applying advanced processing techniques, and using innovative magnetic materials. By continuously improving the magnetic properties of soft ferromagnetic materials, we can expect to see further enhancements in the efficiency and performance of electrical machines in the future [58–98].

2.1.1. Thin Electrical Steel Sheets

The core loss in electrical machines is caused by the varying magnetic flux in the core materials, consisting of hysteresis loss, eddy current loss, and anomalous loss. The eddy current loss is proportional to the square of the current frequency, which is in linear relation with the motor speed. Thus, the eddy current loss in a high-speed motor may be significant. Using thin electrical steel sheets is an effective way to reduce eddy current loss, as it is inversely proportional to the square of the sheet thickness. Enokizono et al. designed a high-efficiency, high-power-density, and high-speed motor using an ultra-thin electrical steel with 80 μm thickness. However, the magnetic flux density in an electrical machine is rotational and not aligned with the field strength. Therefore, the vector magnetic properties of ultra-thin steel sheets need to be measured and modeled for accurate motor design [58].

Pei et al. also investigated the use of thin-gauge non-grain-oriented silicon steels with various thicknesses in EV electric motors and their impact on electromagnetic and mechanical properties and core loss numerical models [59]. Huynh and Hsieh [60] studied the effect of thin electrical steel sheets on the performance of interior PMSMs for EV traction. While thinner sheets may reduce power loss, they may also decrease output torque due to the lower saturation flux density. Additionally, using thin sheet laminations may increase manufacturing difficulty and cost.

2.1.2. High Silicon Electrical Steel Sheets

To reduce eddy current loss, high resistivity electrical steel sheets have been developed by increasing the silicon content. Hasegawa et al. [61] used a high silicon steel, Super E-Core, in 2002 to improve the efficiency of an SRM. A comparison was made with a test machine that used conventional low core loss silicon steel 35A300 as its core to demonstrate the lower power loss of the high silicon steel. Ou et al. [62] designed a high-speed interior PMSM in 2019 using a high silicon steel 10JNEX900 (6.5% Si) as the rotor core. The electromagnetic and mechanical properties of the 10JNEX900 electrical steel were tested. Ma et al. [63] studied the power loss of the motor stator core with the high silicon steel 10JNEX900 in 2002, taking into account the effects of temperature and compressive stress.

High silicon electrical steel sheets feature high resistivity, near-zero magnetostriction, and high magnetic permeability, making them attractive for electromagnetic device applications. However, due to the high silicon content, these materials can become very brittle and difficult to manufacture.

2.1.3. Amorphous Ferromagnetic Metal

The high efficiency and low core loss of amorphous metal (AM), particularly amorphous ferromagnetic metal, make it an attractive material for high-speed electric motors [64]. Various types of motors have been developed using AM as the core material. In 1992, Jensen et al. [65] reported a low loss axial-flux permanent magnet brushless DC motor with tape wound amorphous iron as the stator core. To simplify manufacturing and reduce costs, the stator core is constructed by winding the AM tapes in a toroidal form to minimize eddy current loss. In 2010, Z. Wang et al. [66] designed an axial-flux PMSM with tape wound amorphous core, investigating different core structures for low core loss. In 2011, L. Wang et al. [67] discussed high-efficiency and high-power-density AM-based motors for EVs.

Recent studies have focused on improving AM motor performance. In 2014, Fan et al. [68] developed a high-power-density electric motor with AM core, which demonstrated higher efficiency than a baseline motor with non-oriented silicon steel. However, optimization design is necessary to ensure optimal performance under all conditions. In 2016, Tong et al. [69] analyzed core loss in a permanent magnet synchronous motor with AM core by numerical computation and experiment. In 2019, Tomioka and Akatsu [70] designed a high-speed SRM with AM core for EV application, using a divided rotor structure to reduce eddy current and windage loss. In 2020, Li et al. [71] studied an in-wheel axial-field electric motor with AM stator core for a solar-powered EV, employing a multi-physics design approach for improved multi-objective performance. In 2021, Fan et al. [72] designed and analyzed a high-speed induction motor with AM cores, focusing on low-loss magnetic materials and reliable rotor structures.

Despite these achievements, the widespread use of AM materials in electric motors is still limited. AM is typically in the form of thin continuous ribbon, which is hard and brittle, making it difficult and expensive to manufacture magnetic cores using conventional methods. Additionally, the low-loss property may deteriorate during the production process.

2.1.4. Soft Magnetic Composite

Soft magnetic composite (SMC) materials have unique properties, such as insulation coating on each particle resulting in very low eddy current loss, relatively low total core loss at medium and higher frequencies, magnetic and thermal isotropy due to their powdered nature, and the prospect of low-cost mass production by using powder metallurgical techniques. Over the past three decades, the development of SMC materials and their applications in electromagnetic devices have been significant [73–92]. Various types of electric motors with SMC cores have been designed, analyzed, and prototyped, and some have been applied in practical drives, such as the permanent magnet motor designed by Jack et al. [77] in 1999 for driving an electric bicycle. Axial field motors [78–80], claw pole motors [81–86], and transverse flux motors [87–92] are other examples of machines that have

utilized SMC as the core material, as these machines typically have a three-dimensional magnetic field, making SMC an ideal candidate as a core material.

Despite the unique benefits of SMC materials, there are also some drawbacks. For instance, the magnetic permeability of SMC is quite low, and its mechanical strength is not as high as conventional silicon steel. While molding techniques have been expected to make the fabrication of SMC cores easier, there are still challenging issues, such as the core size and shape against manufacturing productivity and cost, as well as the mass density and uniformity of the molded parts.

2.2. Magnetic Properties of SMC

Because the SMC powder particles are coated with surface insulation and bonding adhesive, the eddy current loss is almost ignorable, implying that the material can operate with higher frequency. This property agrees well with the development of high-power-density electric motors, in which the output power is basically in a linear relation with the operational speed or frequency.

SMC materials have several advantages over conventional electrical machine core materials, including low eddy current loss, isotropy, and the ability to be manufactured into complex structures, making them an ideal choice for high-speed electrical machine design. As shown in Figure 1, the iron loss of different types of motor stator core materials varies with the working frequency [93]. Compared to silicon steel sheets, stators based on amorphous alloy can achieve a much lower iron loss. However, the batch manufacturing technology for amorphous alloy stamping is limited to simple non-slot structures. SMC materials can be a suitable alternative for the stator cores in high-speed permanent magnet machines. When the motor's working frequency is higher than 2000 Hz, SMC can outperform electrical steels in reducing core loss, which in turn helps reduce winding heating.
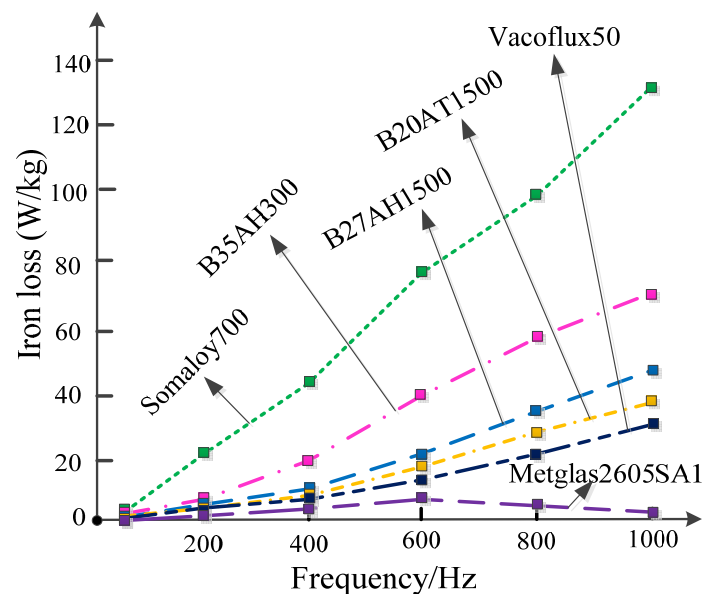

Figure 1. Iron loss of different core materials with respect to frequency.

In 2014, Maloberti et al. [94] presented magnetic modeling for an axial field PM motor utilizing SMC core in EVs. The following year, in 2015, Kobler et al. [95] developed an axial motor with SMC core and ferrite magnets, which showed promising potential for a low-cost, high-power-density design without the use of rare-earth PM. More recently, in 2021, Du et al. [96] presented a claw pole motor that utilized SMC cores. Their research on the SMC preparation process demonstrated that the best magnetic and mechanical properties were achieved with a pressing pressure of 700 MPa and an annealing temperature of 500 °C. In 2022, Chu et al. [97] conducted an analysis on a PM claw pole motor with SMC core,

taking into consideration the material characteristics over a wide range of temperatures. Further, in 2022, Li et al. [98] conducted a study on a flux reversal claw pole SMC motor to minimize cogging torque.

2.3. Conducting Materials

The copper loss, caused by the current flowing in the winding, is typically the largest power loss in an electrical machine. It can be calculated by multiplying the winding resistance with the square of the current. To reduce copper losses, researchers have explored conducting materials with low or zero resistivity, such as superconductors. High-temperature superconductors (HTSs) have been particularly promising for electric motors as they can operate at higher temperatures than low-temperature superconductors, such as those cooled with liquid nitrogen. This makes them more practical and cost-effective for real-world applications. As a result, several HTS electric motors have been developed [99–104].

In 2005, Snitchler et al. [99] presented a 5 MW HTS ship propulsion motor featuring high power density, efficiency, and low noise operation. In 2012, Gonzalez-Parada et al. [100] demonstrated increased power capability by applying HTS BSCOO tapes to the rotor of an axial field induction motor. Moreover, also in 2012, Jin et al. [101] designed a double-sided HTS linear synchronous motor integrated with HTS magnetic suspension, combining the advantages of HTS linear drive and HTS maglev technologies. In 2016, Moon et al. [102] developed a 5 MW 2G HTS motor for ship propulsion, focusing on the rotor with HTS coil, damper, torque disk, and hollow shaft. In 2018, Liu et al. [103] designed a high-speed HTS induction motor with a saddle-shaped HTS armature winding and analyzed its electromagnetic characteristics. In 2021, Zanegin et al. [104] investigated the 2G AC losses in HTS coils of electrical machines under various conditions.

Despite the significant progress made in HTS electric motors, they still face challenges in terms of commercial viability. The design of HTS windings and cooling systems remains complex, and the cost of HTS motor drives is still high, both in terms of initial production and operational expenses. As a result, researchers are continuing their efforts to develop more cost-effective HTS materials and motors.

3. Advanced Modeling and Analysis

Numerous studies have explored the use of advanced electromagnetic materials in electric motors by replacing conventional electrical steel cores. However, simply swapping out the core material is not enough to enhance motor performance. To fully benefit from the new materials, meticulous design optimization that takes into account the unique properties of these materials is crucial. Unfortunately, the property mechanism and mathematical modeling of these new materials have not been fully investigated, particularly in situations where the electric motor experiences two-dimensional (2D) or three-dimensional (3D) vectorial magnetic fluxes. As a result, there is a need to thoroughly study the properties of these materials under 2D and 3D vectorial magnetizations to fully exploit their potential benefits [105–129].

3.1. Measurement of Magnetic Properties under 2D/3D Vectorial Magnetization

Some research projects have been done with the measurement of vectorial magnetic properties, i.e., the relations between magnetic flux density (B) and field strength (H) and the associated core loss under 2D and 3D rotational fluxes for various electromagnetic materials, such as electric steel sheet [105–111], SMC [113–117], amorphous ferromagnetic metal [118,119], and HTS [118,119] materials.

For example, in 1984, Brix et al. [105] presented a method for investigating the rotational magnetization process in electrical steel sheets based on a 2D magnetic measurement apparatus. In 1990, Sievert [106] summarized the advances in 1D alternating and 2D rotational magnetic measurement techniques for electrical steel sheet. Various methods are used for determining the rotational power loss and it was found that the field sensing methods are more convenient and versatile than the thermometric methods, yielding more

information. In 1993, Zhu and Ramsden [107] improved the measurement accuracy of 2D magnetic field in a single-sheet square sample core loss measuring system, in which a novel sandwich structure of sensing coils was proposed. In 1997, Enokizono and Tanabe [108] studied a simplified rotational loss tester, which can be used for any sized sample sheet. In 2014, Appino et al. [109] measured the rotational core loss in non-oriented Fe-Si and Fe-Co sheets up to kilohertz range. In 2016, Li et al. [110] measured the core loss of silicon steel laminations by using a 3D magnetic tester. In 2019, Boubaker et al. [111] reported the design and measurements of a rotational core loss tester, ensuring the rotating flux density vector and uniform distribution in the sample.

As described in Section 2.1.4, SMC materials are very suitable for designing electric motors with 3D magnetic fluxes, and a lot of research has been done on the 2D and 3D magnetic property measurements of SMC [112–116]. Figure 2 shows the experimental results of the magnetization curves obtained with the SMC samples under various magnetization patterns, by using the developed 3D magnetic testing system shown in Figures 3 and 4 [117,118].

In 2021, Sarker et al. [119,120] measured the rotational core loss of a Fe-based amorphous magnetic material by using a square specimen tester (SST) as shown in Figure 5. The 2D rotational magnetic fluxes are generated by the currents flowing in the two sets of excitation coils wound on X- and Y-axis magnetic poles.

Some rotational magnetic property measurements have also been carried out on HTS materials. Soomro et al. [121,122] reported their experimental setup and measurement results of AC loss in HTS YBCO bulks by modifying the 2D magnetic testing system as shown in Figure 6. For experiment purposes, the HTS sample was cooled down to the superconducting mode in a liquid nitrogen box.

The large amount of data of magnetic properties measured under 2D and 3D vectorial magnetizations are necessary for in-depth understanding of the core loss mechanism and proper mathematic modeling for designing various electric motors.
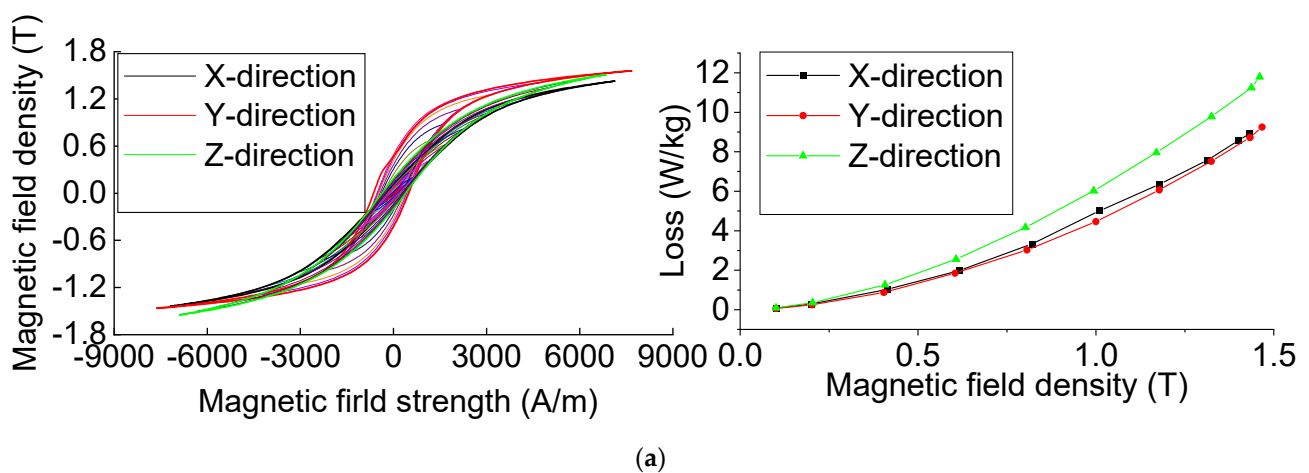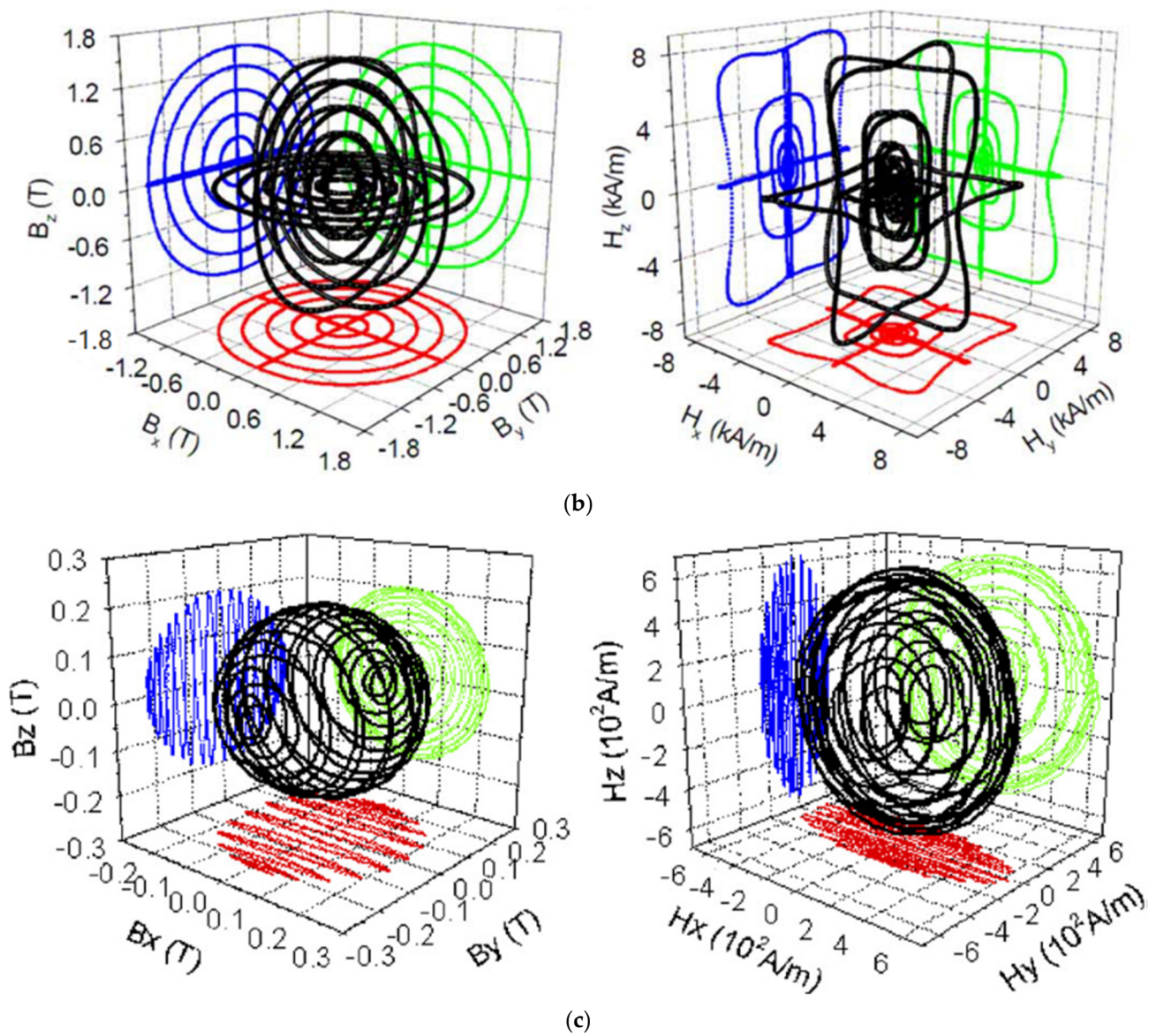

(a)

Figure 2. *Cont*.

(b)

(c)

Figure 2. Experimental results of SMC samples at 50 Hz: (**a**) B-H relation and associated core loss under 1D alternating sinusoidal B; (**b**) B-H relation under 2D circularly rotating B; and (**c**) B-H relation under 3D spherical B.
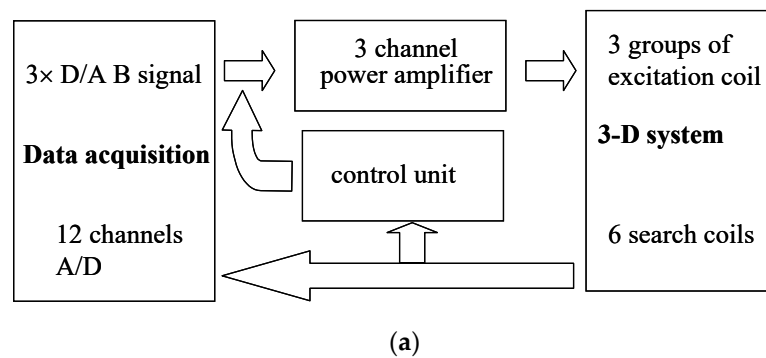

(a)

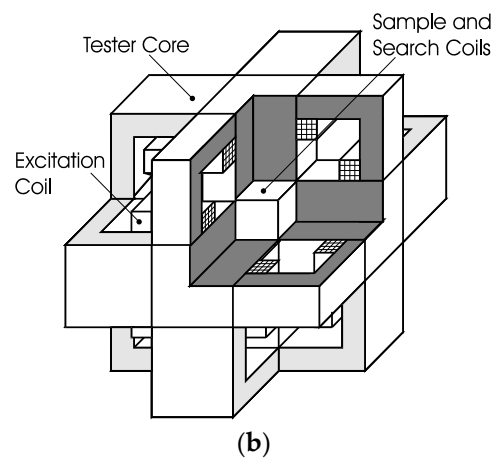**Figure 3.** *Cont*.

(b)

Figure 3. A 3D vectorial magnetic property measurement system: (**a**) block diagram, and (**b**) structure of 3D view.
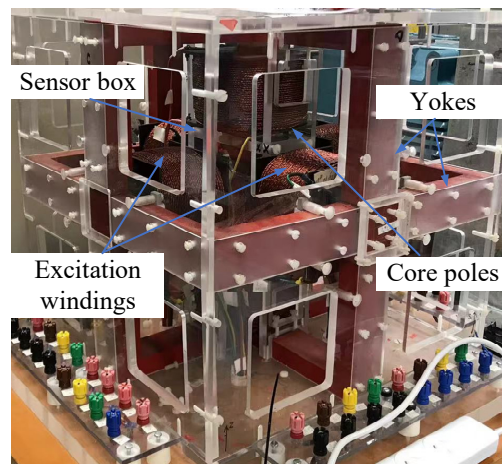

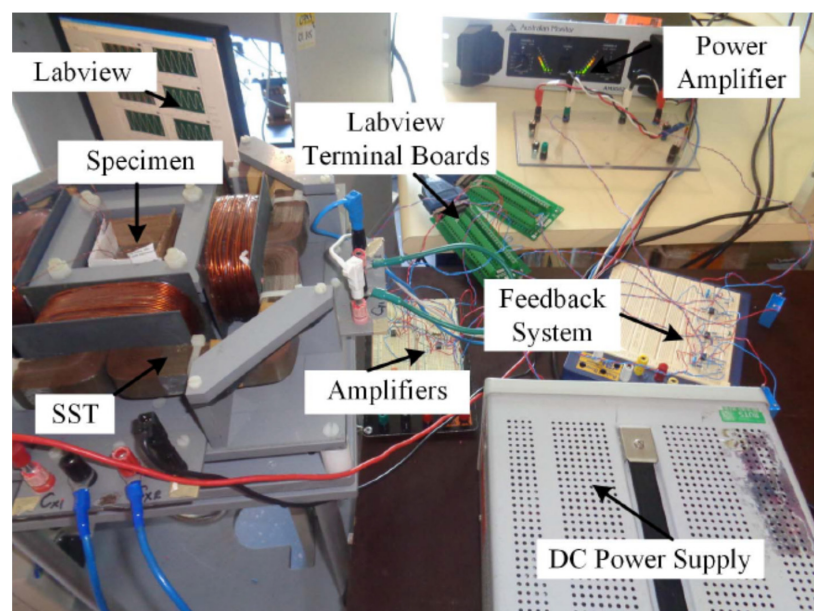**Figure 4.** A photo of the 3D vectorial magnetic property measurement system.

Figure 5. Photo of the 2D vectorial magnetic property measurement system.
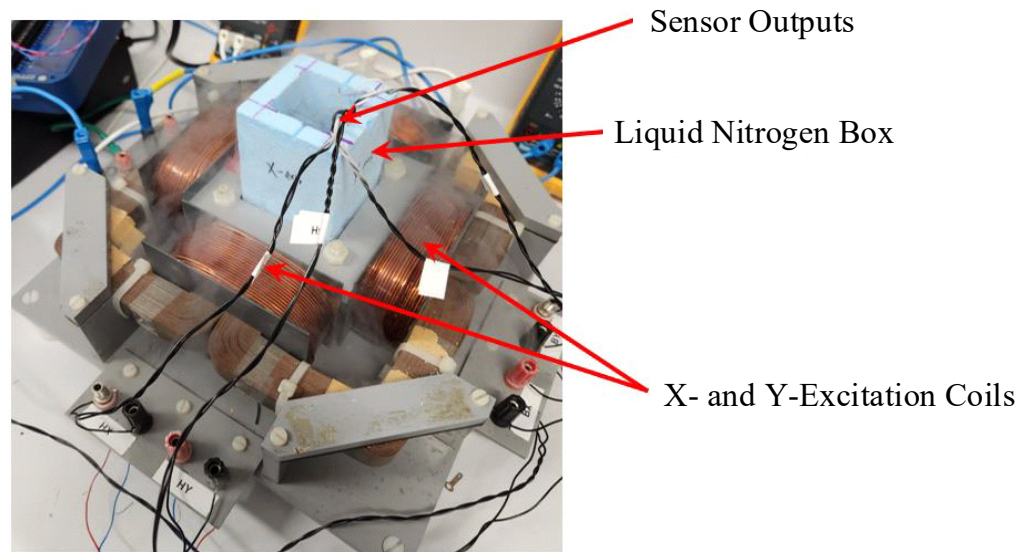
Figure 6. Photo of the 2D magnetic property measurement system for HTS samples.

3.2. Modeling of 2D/3D Vectorial Magnetic Properties

Based on the measured magnetic properties including the relations between **B** (magnetic flux density) and **H** (magnetic field strength) vectors, and associated core loss, some mathematical models of the 2D/3D vectorial magnetic properties have been established, which are essential for magnetic field analysis of electric motors.

Because of the vectorial rotational magnetization, there is generally a phase difference between the **B** and **H** vectors, and their relationship should be described in a matrix form as below [123–128]:

$$H_i = \sum_j v_{ij} B_j \tag{1}$$

where v_{ij} is the reluctivity matrix ($i,j = x,y,z$ in rectangular coordinate or $i,j = r,\theta,z$ in cylindrical coordinate). According to the Maxwell's equations, in magnetic static field analysis, the relation between magnetic vector potential A and the applied current density vector J_0 can be derived as

$$\nabla \times (v \nabla \times A) = J_0. \tag{2}$$

In rectangular coordinates, the equation for the x-component of J_0 can be written as (3). The equations for J_y and J_z can be derived in a similar way.

$$\frac{\partial}{\partial y} \left[v_{zx} \left(\frac{\partial A_z}{\partial y} - \frac{\partial A_y}{\partial z} \right) + v_{zy} \left(\frac{\partial A_x}{\partial z} - \frac{\partial A_z}{\partial x} \right) + v_{zz} \left(\frac{\partial A_y}{\partial x} - \frac{\partial A_x}{\partial y} \right) \right]$$
$$- \frac{\partial}{\partial z} \left[v_{yx} \left(\frac{\partial A_z}{\partial y} - \frac{\partial A_y}{\partial z} \right) + v_{yy} \left(\frac{\partial A_x}{\partial z} - \frac{\partial A_z}{\partial x} \right) + v_{yz} \left(\frac{\partial A_y}{\partial x} - \frac{\partial A_x}{\partial y} \right) \right] = J_x \tag{3}$$

Different measurements of magnetic materials have indicated that the behavior of core loss under vectorial rotational magnetization is distinct from that observed under alternating magnetic flux. An example of this is demonstrated in Figure 7, where the core loss of an SMC sample was measured under varying peak values and frequencies of flux densities, for both alternating and purely rotational magnetizations [114].

It is evident that rotational core loss behaves differently than its alternating counterpart, and thus requires novel and appropriate models to be proposed. When an electrical machine rotates, the magnetic flux density B vector at any given location on the core typically forms a 3D irregular locus [129]. The B components projected onto the three coordinate axes are periodic functions of time, which can be decomposed into fundamental and harmonic terms using Fourier series. For each harmonic order, including the fundamental, the three components form an elliptical locus on a plane that may not align with any major coordinate

plane, such as the XoY, YoZ, or ZoX plane. Previous research has shown that the total core loss can be obtained by summing up the losses contributed by all harmonics [120,129].

Several new models have been proposed to account for the rotational core loss in electrical machines, as discussed in references [130–132]. These models have been developed based on measured data obtained from material samples exposed to both alternating and circularly rotating magnetizations.
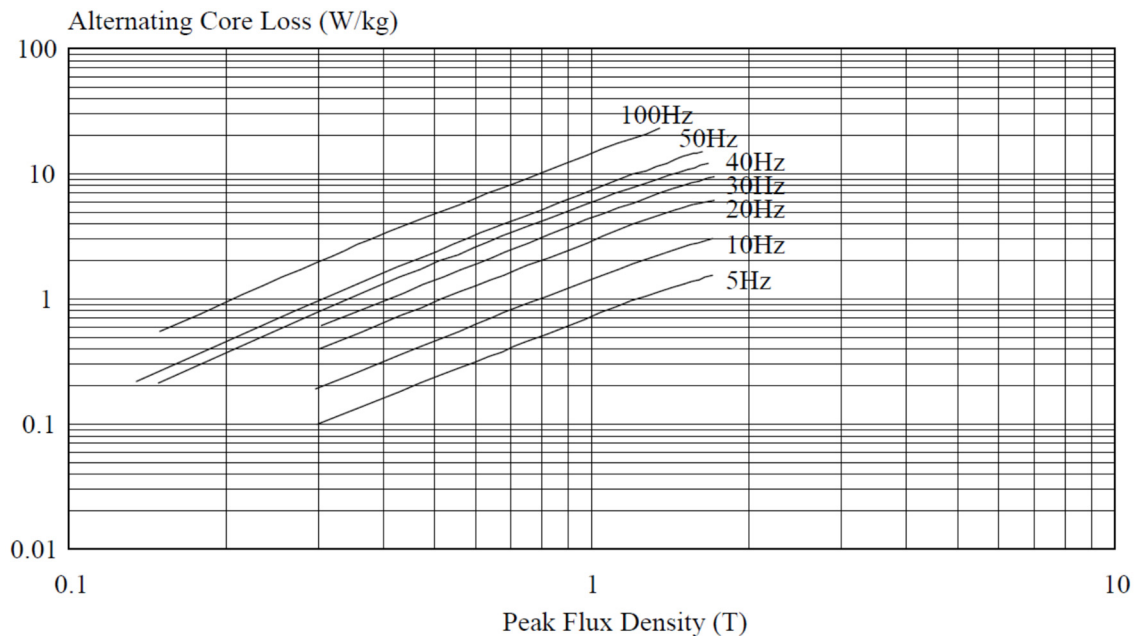
(a)
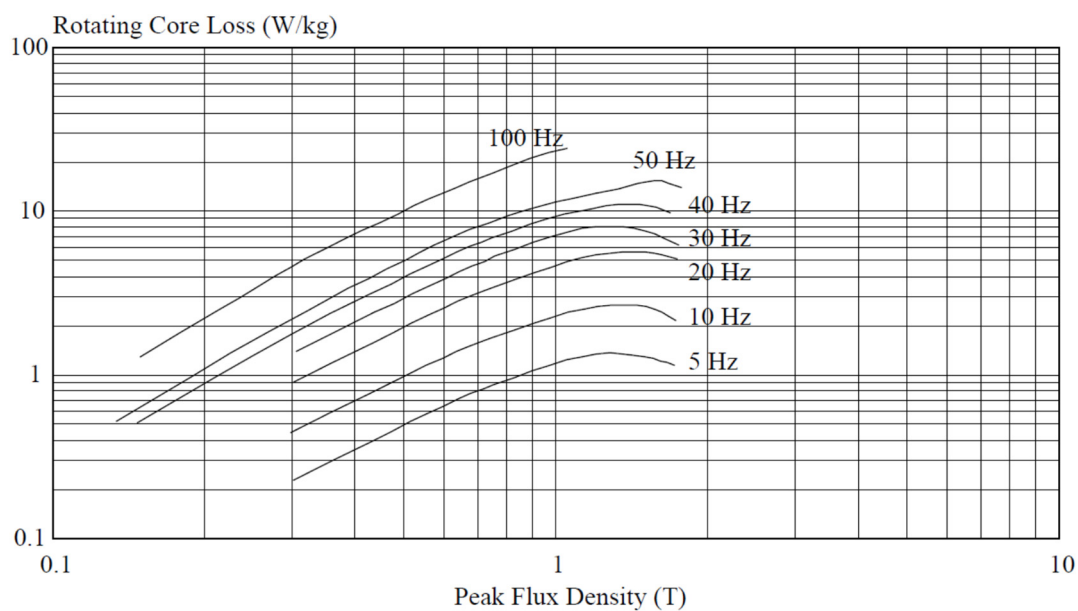
(b)

Figure 7. Measured core losses of an SMC sample under (**a**) alternating and (**b**) circularly rotating magnetizations with different peak values and frequencies of flux density.

3.3. Applications of 2D/3D Rotational Core Loss Models

According to references [130–132], it may be sufficient for material suppliers to provide data for 1D alternating and 2D purely circular flux densities of various peak values and

frequencies. In 1991, Bertotti et al. [130] employed the common three-term model [133] to calculate the core loss of an induction motor. The hysteresis loss with an ellipsoidal rotating flux density was estimated using linear interpolation between alternating and rotational core losses. However, this interpolation method is a rough approximation. In 1994, Zhu et al. [134] improved the accuracy of the prediction by deriving an elliptically rotational core loss formula, given by Equation (4). In this formula, P_t represents the core loss caused by an ellipsoidal rotating **B**, P_r is the corresponding loss due to a circularly rotating **B** with the same peak value and frequency, and P_a is due to an alternating **B**. Additionally, R_B denotes the axis ratio of the ellipsoidal **B**.

$$P_t = R_B P_r + (1 - R_B)^2 P_a \tag{4}$$

In 1998, Zhu and Ramsden [131] proposed enhanced models for computing the rotational core losses of electrical machines, where the rotational hysteresis loss P_{hr} is computed using Equations (5) and (6), where f, B_P, and B_s are, respectively, the frequency, peak value, and saturated value of flux density, and a_1, a_2, and a_3 are coefficients. These models were employed to estimate the core loss of a PM motor and achieved better accuracy. In 2005, Guo et al. [132] applied this improved model to calculate the core loss of a PM claw pole motor with an SMC stator core, resulting in a high level of accuracy when compared with experimental data obtained from a motor prototype.

$$\frac{P_{hr}}{f} = a_1 \left[\frac{\frac{1}{s}}{\left(a_2 + \frac{1}{s}\right)^2 + a_3^2} - \frac{\frac{1}{(2-s)}}{\left[a_2 + \frac{1}{(2-s)}\right]^2 + a_3^2} \right] \tag{5}$$

$$s = 1 - \frac{B_P}{B_s} \sqrt{1 - \frac{1}{a_2^2 + a_3^2}} \tag{6}$$

where f is the field excitation frequency, B_P the magnitude of the circular B vector, B_s the saturation flux density. A_1, a_2, and a_3 are all coefficients that can be obtained by curve-fitting the data.

4. Advanced Design and Optimization

As new materials have both advantages and disadvantages, a system-level design approach is necessary to maximize the benefits while minimizing the drawbacks. However, electric motor drives are complex systems that consist not only of the motor but also of the power electronic converter and controller. Even within the motor itself, there are numerous components with multi-physics considerations such as electromagnetic, thermal, and mechanical aspects. Furthermore, many factors, such as material properties, are nonlinear, and motor parameter and performance calculations are highly time-consuming, especially when accurate determination requires 3D finite element analysis. Additionally, design optimization necessitates numerous iterations.

To address these challenges, researchers have developed and applied the so-called multi-level, multi-objective, and multi-physics optimization technique in the design and analysis of electric motor drive systems [135–156]. This approach enables designers to consider multiple levels of the motor drive system, including the motor, converter, and controller, as well as the numerous interdependent physics involved. The MMM optimization technique also allows for the consideration of multiple objectives, such as efficiency, power density, cost, and reliability, to achieve an optimal design.

Many researchers have applied the MMM optimization technique in their studies. For instance, Knorr et al. [135] introduced a multi-level modeling methodology for analyzing a claw pole alternator, considering the trade-off between simulation efficiency and accuracy. Guo et al. [136] applied the multi-level multi-domain modeling for designing a transverse flux motor, in which a two-level hierarchical design architecture is constructed. This ap-

proach appears to be effective, with fast calculation and good accuracy. Wang et al. [137] conducted multi-level optimization of a permanent magnet motor by using a multi-level genetic algorithm. Lei et al. [138] carried out the system-level design of a transverse flux motor drive system with the six sigma robust optimization technique included. Lei et al. presented their studies on the system-level design optimization of electric motor drive systems using the traditional deterministic approach [139], and the robust approach considering parameter uncertainty [140]. They also summarized the key techniques of multi-level design optimization for permanent magnet motors [141]. Asef et al. reported a rotor shape multi-level design optimization for a permanent magnet synchronous motor, aiming to reduce the mechanical stress in the rotor core [142]. Meng et al. [143] conducted the multi-level optimization of a flux-modulated machine based on machine learning techniques.

Apart from multi-level design optimization, extensive research has also been conducted on multi-objective optimization [144–148], as well as multi-physics or multi-disciplinary optimization of electric motors [149–151]. Recently, some research has focused on the mutual effects of multi-disciplinary factors, such as the dynamic two-way effects among power loss, operational temperature, and mechanical stress [152–156]. This technique is among the basis for developing digital twin models of electric motor drives [157–160].

In conclusion, the MMM optimization technique is an effective tool for designing and analyzing electric motor drive systems. Researchers have successfully applied the technique to optimize various types of motors, and the approach has evolved to include multi-objective and multi-physics optimization. Additionally, recent research work has focused on the mutual effects of multi-disciplinary factors, contributing to the development of digital twin models of electric motor drives.

5. Discussions and Conclusions

This paper provides an overview of advanced design and analysis techniques used to develop high-power-density electric motors for electric vehicles. The techniques include the application of novel electromagnetic materials, advanced characterization of material properties under motor operational conditions, and accurate mathematical modeling. The paper also discusses the use of system-level multi-physics optimization for achieving optimal system performance.

5.1. Remaining Challenges

Despite significant progress in research and industrial applications, there are still several challenging tasks that require attention in the future development of high-power-density electric motors in EVs. These include:

(1) The lack of sufficient fundamental property data for electromagnetic materials, such as the relationship between magnetic field strength and flux density under various conditions such as magnetization patterns, magnitudes, frequency, temperature, mechanical stress, DC bias, and magnetostriction;

(2) The need for system-level design optimization of the entire PMSM drive system for optimal performance since assembling individually optimal components such as motor and inverter cannot guarantee optimal system performance. The interaction of multiphysics effects, such as thermal and stress characteristics, should also be considered to improve the accuracy of iron loss prediction for PMSMs, reducing computational cost and providing better accuracy;

(3) The importance of using new materials or high-quality manufacturing in EV drive systems design optimization. New materials such as SMC have great potential for designing electrical machines with high performance and/or low-cost and novel topologies. Future robust design optimization should fully consider manufacturing tolerances, material diversities, and assembling errors to present a comprehensive solution for high quality manufacturing and design;

(4) The need for effective control circuit design for dynamic and steady-state performances of PMSM drive systems. Traditional control algorithms including field-

oriented control (FOC), direct torque control (DTC), and model predictive control (MPC) have been developed and employed successfully, but are challenging to guarantee satisfactory performance in the presence of parameter uncertainties and external disturbances during changing operating conditions. Future development should focus on coordinated control strategies at both system and subregion levels;

(5) The challenge of achieving effective modeling with sufficient accuracy and reasonable computation speed using existing mathematical models of material properties. There is a trend towards designing electric motors and drives with digital twin (DT)-based models, optimizing motor performance, as well as manufacturing and operation processes throughout the entire cycle of motor life.

5.2. Comparison between Vectorial Magnetic Properties and Conventional Alternating Properties

Vectorial magnetic properties refer to the magnetic behavior of materials under different vectorial rotational magnetic fields. This approach differs from traditional alternating magnetic properties, which only consider the behavior of materials under a sinusoidal magnetic field in one direction. Vectorial magnetic properties are particularly relevant in the context of electrical machines, as they can provide a more accurate representation of the materials' behavior under rotational magnetic conditions. However, one of the challenges of using vectorial magnetic properties is the complexity of the characterization process. Traditional alternating magnetic properties can be measured using simple laboratory equipment, while vectorial magnetic properties require more advanced measurement techniques and analysis tools, which can increase the cost and time required for the characterization process. Despite these challenges, vectorial magnetic properties offer a more comprehensive understanding of the magnetic behavior of materials, and are becoming increasingly important in the design and development of high-performance electrical machines. Nevertheless, traditional alternating magnetic properties are still widely used due to their simplicity and ease of measurement.

5.3. Benefits

This paper offers an overview of advanced magnetic materials and their applications in designing high-power-density electric motors for electric vehicles, with a key focus on the benefits of vectorial rotational magnetic properties. By exploring these properties, the paper contributes to the development of more accurate mathematical models for predicting the performance of electric motors. Optimized design based on these models can lead to improved efficiency, power density, and reliability of electric motors. Additionally, this paper highlights the potential advantages of using various advanced electromagnetic materials. The emphasis on vectorial rotational magnetic properties and advanced materials underscores the potential for future progress in the field and the advancement of more efficient and reliable electric vehicles.

Abbreviations

AM	Amorphous metal
DT	Digital twin
DTC	Direct torque control
2D	Two-dimensional
3D	Three-dimensional
EV	Electric vehicle
FOC	Field-oriented control
HTS	High-temperature superconductor
MMM	Multi-level, multi-objective, multi-disciplinary
MPC	Model predictive control
PM	Permanent magnet
PMSM	Permanent magnet synchronous motor
PV	Photovoltaic
SRM	Switched reluctance motor
Syn-RM	Synchronous reluctance motor
SST	Square specimen tester

References

1. Islam, M.R.; Guo, Y.G.; Zhu, J.G. A Review of Offshore Wind Turbine: Technical Challenges, and Research and Development Trends. *Renew. Sustain. Rev.* **2014**, *33*, 161–176. [CrossRef]
2. Yin, W.; Dong, Z.; Liu, L.; Rui, X. Self-stabilising Speed Regulating Differential Mechanism for Continuously Variable Speed Wind Power Generation System. *IET Renew. Power Gener.* **2020**, *14*, 3002–3009. [CrossRef]
3. Bosnjakovic, M.; Katinic, M.; Santa, R.; Maric, D. Wind Turbine Technology Trends. *Appl. Sci.* **2022**, *12*, 8653. [CrossRef]
4. Islam, M.R.; Guo, Y.G.; Zhu, J.G. A Multilevel Medium-Voltage Inverter for Step-up-Transformerless Grid Connection of Photovoltaic Power Plants. *IEEE J. Photovolt.* **2014**, *4*, 881–889. [CrossRef]
5. Shafiullah, M.D.; Ahmed, S.D.; Al-sulaiman, F.A. Grid Integration Challenges and Solution Strategies for Solar PV Systems: A Review. *IEEE Access* **2022**, *10*, 52233–52257. [CrossRef]
6. Su, W.; Rahimi-Eichi, H.; Zeng, W.; Chow, M.-Y. A Survey on the Electrification of Transportation in a Smart Grid Environment. *IEEE Trans. Ind. Inform.* **2012**, *8*, 1–10. [CrossRef]
7. Viswanath, A.; Farid, A.M. A Hybrid Dynamic System Model for the Assessment of Transportation Electrification. In Proceedings of the 2014 American Control Conference, Portland, OR, USA, 4–6 June 2014; pp. 4617–4623.
8. Arias-Londono, A.; Gil-Gonzalez, W.; Montoya, O. A Linearized Approach for the Electric Light Commercial Vehicle Routing Problem Combined with Changing Station Siting and Power Distribution Network Assessment. *Appl. Sci.* **2021**, *11*, 4870. [CrossRef]
9. Fernandes, J.F.P.; Bhagubai, P.P.C.; Branco, P.J.C. Recent Developments in Electrical Machine Design for the Electrification of Industrial and Transportation Systems. *Energies* **2022**, *15*, 6390. [CrossRef]
10. Lin, J.; Schofield, N.; Emadi, A. External-Rotor 6–10 Switched Reluctance Motor for an Electric Bicycle. *IEEE Trans. Transp. Electrif.* **2015**, *1*, 348–356. [CrossRef]
11. Yang, Y.; Rahman, M.; Lambert, T.; Bilgin, B.; Emadi, A. Development of an External Rotor V-Shape Permanent Magnet Machine for E-Bike Application. *IEEE Trans. Energy Convers.* **2018**, *33*, 1650–1658. [CrossRef]
12. Son, J.-C.; Lim, D.-K. Novel Stator Core of the Permanent Magnet Assisted Synchronous Reluctance Motor for Electric Bicycle Traction Motor Using Grain-Oriented Electrical Steel. In Proceedings of the 2021 24th International Conference on Electrical Machines and Systems (ICEMS), Gyeongju, Republic of Korea, 31 October–3 November 2021; pp. 1215–1218.
13. Conto, C.; Bianchi, N. E-Bike Motor Drive: A Review of Configurations and Capabilities. *Energies* **2023**, *16*, 160. [CrossRef]
14. Zhu, Z.Q.; Howe, D. Electrical Machines and Drives for Electric, Hybrid, and Fuel Cell Vehicles. *Proc. IEEE* **2007**, *95*, 746–765. [CrossRef]
15. Takahashi, T.; Takemoto, M.; Ogasawara, S.; Hino, W.; Takezaki, K. Size and Weight Reduction of an In-Wheel Axial-Gap Motor Using Ferrite Permanent Magnets for Electric Commuter Cars. *IEEE Trans. Ind. Appl.* **2017**, *53*, 3927–3935. [CrossRef]
16. Sun, X.; Shi, Z.; Lei, G.; Guo, Y.; Zhu, J.G. Analysis and Design Optimization of a Permanent Magnet Synchronous Motor for a Campus Patrol Electric Vehicle. *IEEE Trans. Veh. Technol.* **2019**, *68*, 10535–10544. [CrossRef]
17. Sun, X.; Shi, Z.; Cai, Y.; Lei, G.; Guo, Y.; Zhu, J. Driving-Cycle Oriented Design Optimization of a Permanent Magnet Hub Motor Drive System for a Four-Wheel-Drive Electric Vehicle. *IEEE Trans. Transp. Electrif.* **2020**, *6*, 1115–1125. [CrossRef]
18. Bruzinga, G.R.; Sguarezi Filho, A.J.; Pelizari, A. Analysis and Design of 3 kW Axial Flux Permanent Magnet Synchronous Motor for Electric Car. *IEEE Trans. Lat. Am.* **2022**, *20*, 855–863. [CrossRef]
19. Ritari, A.; Vepsalainen, J.; Kivekas, K.; Tammi, K.; Laitinen, H. Energy Consumption and Lifecycle Cost Analysis of Electric City Buses with Multispeed Gearboxes. *Energies* **2020**, *13*, 2117. [CrossRef]

20. Xu, Y.; Ai, M.; Xu, Z.; Liu, W.; Wang, Y. Research on Interior Permanent Magnet Synchronous Motor Based on Performance Matching of Electric Bus. *IEEE Trans. Appl. Supercond.* **2021**, *31*, 5204304. [CrossRef]
21. Guo, Y.; Jin, J.X.; Zhu, J.G.; Lu, H.Y. Design and Analysis of a Prototype Linear Motor Driving System for HTS Maglev Transportation. *IEEE Trans. Appl. Supercond.* **2007**, *17*, 2087–2090.
22. Ikeda, R.; Yusya, S.; Kondo, K. Study on Design Method for Increasing Power Density of Induction Motors for Electric Railway Vehicle Traction. In Proceedings of the 2019 IEEE International Electric Machines & Drives Conference (IEMDC), San Diego, CA, USA, 12–15 May 2019; pp. 1545–1550.
23. Chen, H.; Jiang, B.; Chen, W.; Yi, H. Data-driven Detection and Diagnosis of Incipient Faults in Electrical Drives of High-Speed Trains. *IEEE Trans. Ind. Electron.* **2019**, *66*, 4716–4725. [CrossRef]
24. Hansen, J.F.; Wendt, F. History and State of the Art in Commercial Electric Ship Propulsion, Integrated Power Systems, and Future Trends. *Proc. IEEE* **2015**, *103*, 2229–2242. [CrossRef]
25. Sulligoi, G.; Vicenzutti, A.; Menis, R. All-Electric Ship Design: From Electrical Propulsion to Integrated Electrical and Electronic Power Systems. *IEEE Trans. Transp. Electrif.* **2016**, *2*, 507–521. [CrossRef]
26. Fang, S.; Wang, Y.; Gou, B.; Xu, Y. Toward Future Green Maritime Transportation: An Overview of Seaport Microgrids and All-Electric Ships. *IEEE Trans. Veh. Technol.* **2020**, *69*, 207–219. [CrossRef]
27. Masson, J.; Luongo, C.A. High Power Density Superconducting Motor for All-Electric Aircraft Propulsion. *IEEE Trans. Appl. Supercond.* **2007**, *15*, 2226–2229. [CrossRef]
28. Sarlioglu, B.; Morris, C.T. More Electric Aircraft: Review, Challenges, and Opportunities for Commercial Transport Aircraft. *IEEE Trans. Transp. Electrif.* **2015**, *1*, 54–64. [CrossRef]
29. Tom, L.; Khowja, M.; Vakil, G.; Gerada, C. Commercial Aircraft Electrification—Current State and Future Scope. *Energies* **2021**, *14*, 8381. [CrossRef]
30. Benzaquen, J.; He, J.; Mirafzal, B. Toward More Electric Powertrains in Aircraft: Technical Challenges and Advancements. *CES Trans. Electr. Mach. Syst.* **2021**, *5*, 177–193. [CrossRef]
31. Jiang, S.Z.; Chau, K.T.; Chan, C.C. Spectral Analysis of a New Six-Phase Pole-Changing Induction Motor Drive for Electric Vehicles. *IEEE Trans. Ind. Electron.* **2003**, *50*, 123–131. [CrossRef]
32. Xu, W.; Zhu, J.; Zhang, Y.; Li, Y.; Wang, Y.; Guo, Y. An Improved Equivalent Circuit Model of a Single-Sided Linear Induction Motor. *IEEE Trans. Veh. Technol.* **2010**, *59*, 2277–2289. [CrossRef]
33. Mei, J.; Zuo, Y.; Lee, C.H.T.; Kirtley, J.L. Modeling and Optimizing Method for Axial Flux Induction Motor Electric Vehicles. *IEEE Trans. Veh. Technol.* **2020**, *69*, 12822–12831. [CrossRef]
34. Wang, S.; Zhan, Q.; Ma, Z.; Zhou, L. Implementation of a 50-kW Four-Phase Switched Reluctance Motor Drive System for Hybrid Electric Vehicle. *IEEE Trans. Magn.* **2005**, *41*, 501–504. [CrossRef]
35. Xue, X.D.; Cheng, K.W.E.; Ng, T.W.; Cheung, N.C. Multi-Objective Optimization Design of In-Wheel Switched Reluctance Motors in Electric Vehicles. *IEEE Trans. Ind. Electron.* **2010**, *57*, 2980–2987. [CrossRef]
36. Gan, C.; Wu, J.; Sun, Q.; Kong, W.; Li, H.; Hu, Y. A Review on Machine Topologies and Control Techniques for Low-Noise Switched Reluctance Motors in Electric Vehicle Applications. *IEEE Access* **2018**, *6*, 31430–31443. [CrossRef]
37. Patel, N.R.; Shah, V.A.; Lokhande, M.M. A Novel Approach to the Design and Development of 12/15 Radial Field C-Core Switched Reluctance Motor for Implementation in Electric Vehicle Application. *IEEE Trans. Veh. Technol.* **2018**, *67*, 8031–8040. [CrossRef]
38. Sun, X.; Wan, B.; Lei, G.; Tian, X.; Guo, Y.; Zhu, J. Multiobjective and Multiphysics Design Optimization of a Switched Reluctance Motor for Electric Vehicle Application. *IEEE Trans. Ind. Appl.* **2021**, *36*, 3294–3304. [CrossRef]
39. Xu, W.; Lei, G.; Wang, T.; Yu, X.; Zhu, J.; Guo, Y. Theoretical Research on New Laminated Structure Flux Switching Permanent Magnet Machine for Novel Topologic Plug-in Hybrid Electrical Vehicle. *IEEE Trans. Magn.* **2012**, *48*, 4050–4053. [CrossRef]
40. Zhu, X.; Wang, X.; Zhang, C.; Wang, L.; Wu, W. Design and Analysis of a Spoke-Type Hybrid Permanent Magnet Motor for Electric Vehicles. *IEEE Trans. Magn.* **2017**, *53*, 8208604. [CrossRef]
41. Jin, Z.; Sun, X.; Lei, G.; Guo, Y.; Zhu, J.G. Sliding Mode Direct Torque Control of SPMSMs Based on a Hybrid Wolf Optimization Algorithm. *IEEE Trans. Ind. Electron.* **2022**, *69*, 4534–4544. [CrossRef]
42. Bhagubai, P.P.C.; Sarrico, J.G.; Fernandes, J.F.P.; Branco, P.J.C. Design, Multi-Objective Optimization, and Prototyping of a 20 kW 8000 rpm Permanent Magnet Synchronous Motor for a Competition Electric Vehicle. *Energies* **2020**, *13*, 2465. [CrossRef]
43. Lee, H.-S.; Hwang, M.-H.; Cha, H.-R. Electromagnetic Field Analysis and Design of a Hermetic Interior Permanent Magnet Synchronous Motor with Helical-Grooved Self-Cooling Case for Unmanned Aerial Vehicles. *Appl. Sci.* **2021**, *11*, 4856. [CrossRef]
44. Cai, S.; Zhu, Z.Q.; Huang, L.; Qu, H. Comparison of Stator Slot Permanent Magnet Hybrid Excited Machine with Rotor Interior Permanent Magnet Machine for EV/HEV Application. In Proceedings of the 10th International Conference on Power Electronics, Machines and Drives (PEMD 2020), Online, 15–17 December 2020; pp. 645–650.
45. Zheng, P.; Liu, Y.; Wang, Y.; Cheng, S. Magnetization Analysis of the Brushless DC Motor Used for Hybrid Electric Vehicle. *IEEE Trans. Magn.* **2005**, *41*, 522–524. [CrossRef]
46. Naseri, F.; Farjah, E.; Ghanbari, T. An Efficient Regenerative Braking System Based on Battery/Supercapacitor for Electric, Hybrid, and Plug-in Hybrid Electric Vehicles With BLDC Motor. *IEEE Trans. Veh. Technol.* **2017**, *66*, 3724–3738. [CrossRef]

47. Eberleh, B.; Hartkopf, T. A High Speed Induction Machine with Two Speed Transmission as Drive for Electric Vehicles. In Proceedings of the International Symposium on Power Electronics, Electrical Drives, Automation and Motion, Taormina, Italy, 23–26 May 2006; pp. 249–254.
48. Huang, Y.; Zhu, J.; Guo, Y.; Lin, Z.; Hu, Q. Design and Analysis of a High-Speed Claw Pole Motor With Soft Magnetic Composite Core. *IEEE Trans. Magn.* **2007**, *43*, 2492–2494. [CrossRef]
49. Huang, Y.; Zhu, J.; Guo, Y. Thermal Analysis of High-Speed SMC Motor Based on Thermal Network and 3-D FEA with Rotational Core Loss Included. *IEEE Trans. Magn.* **2009**, *45*, 4684–4687.
50. Hosseini, M.S.; Vaez-Zadeh, S. Modeling and Analysis of Linear Synchronous Motors in High-Speed Maglev Vehicles. *IEEE Trans. Magn.* **2009**, *46*, 2656–2664. [CrossRef]
51. Damiano, A.; Floris, A.; Fois, G.; Marougiu, I.; Porru, M.; Serpi, A. Design of a High-Speed Ferrite-Based Brushless DC Machine for Electric Vehicles. *IEEE Trans. Ind. Appl.* **2017**, *53*, 4279–4287. [CrossRef]
52. Dang, L.; Bernard, N.; Bracikowski, N.; Berthiau, G. Design Optimization with Flux Weakening of High-Speed PMSM for Electrical Vehicle Considering the Driving Cycle. *IEEE Trans. Ind. Electron.* **2017**, *64*, 9834–9843. [CrossRef]
53. Credo, A.; Fabri, G.; Villani, M.; Popescu, M. Adopting the Topology Optimization in the Design of High-Speed Synchronous Reluctance Motors for Electric Vehicles. *IEEE Trans. Ind. Appl.* **2020**, *56*, 5429–5438. [CrossRef]
54. Prakht, V.; Dmitrievskii, V.; Kazakbaev, V.; Oshurbekov, S.; Ibrahim, M. Optimal Design of a Novel Three-Phase High-Speed Flux Reversal Machine. *Appl. Sci.* **2019**, *9*, 3822. [CrossRef]
55. Cui, W.; Ren, L.; Zhou, J.; Zhang, Q. A New IPMSM With Hybrid Rotor Structure for Electrical Vehicle With Reduced Magnet Loss. *IEEE Trans. Magn.* **2022**, *58*, 1–6. [CrossRef]
56. Mashrouteh, S.; Khajepour, A.; Kasaiezadeh, A.; Esmailzadeh, E.; Chen, S.K.; Litkouhi, B. Multi-Actuation Controller for Performance Vehicles: Optimal Torque Allocation and Active Aerodynamic. *IEEE Trans. Veh. Technol.* **2022**, *71*, 2721–2733. [CrossRef]
57. Credo, A.; Villani, M.; Fabri, G.; Popescu, M. Adoption of the Synchronous Reluctance Motor in Electric Vehicles: A Focus on the Flux Weakening Capability. *IEEE Trans. Transp. Electrif.* **2023**, *9*, 805–818. [CrossRef]
58. Ueno, S.; Enokizono, M.; Mori, Y.; Yamazaki, K. Vector Magnetic Characteristics of Ultra-Thin Electrical Steel Sheet for Development of High-Efficiency High-Speed Motor. *IEEE Trans. Magn.* **2017**, *53*, 6300604. [CrossRef]
59. Pei, R.; Zeng, L.; Gao, L. Studies of Core Loss of Thin Non-oriented Electrical Steel for Electrical Vehicle Traction Motors. In Proceedings of the 2018 21st International Conference on Electrical Machines and Systems (ICEMS), Jeju, Republic of Korea, 7–10 October 2018; pp. 2715–2718.
60. Huynh, T.; Hsieh, M.-F. Performance Evaluation of Thin Electrical Steels Applied to Interior Permanent Magnet Motor. In Proceedings of the 2016 19th International Conference on Electrical Machines and Systems (ICEMS), Chiba, Japan, 13–16 November 2016.
61. Hasegawa, M.; Tanaka, N.; Chiba, A.; Fukao, T. The Operation Analysis and Efficiency Improvement of Switched Reluctance Motors with High Silicon Steel. In Proceedings of the Power Conversion Conference-Osaka 2002 (Cat. No.02TH8579), Osaka, Japan, 2–5 April 2002; pp. 981–986.
62. Ou, J.; Liu, Y.; Breining, P.; Gietzelt, T.; Gietzelt, T.; Wunsch, T.; Doppelbauer, M. Study of the Electromagnetic and Mechanical Properties of a High-silicon Steel for a High-speed Interior PM Rotor. In Proceedings of the 2019 22nd International Conference on Electrical Machines and Systems (ICEMS), Harbin, China, 11–14 August 2019; pp. 1–4.
63. Ma, D.; Li, J.; Tian, B.; Zhang, H.L.M.; Pei, R. Studies on Loss of a Motor Iron Core with High Silicon Electrical Steel Considering Temperature and Compressive Stress Factors. In Proceedings of the 2022 IEEE 5th International Electrical and Energy Conference (CIEEC), Nangjing, China, 27–29 May 2022; pp. 4243–4248.
64. Sarker, P.C.; Guo, Y.; Lu, H.; Zhu, J. A Generalized Inverse Preisach Dynamic Hysteresis Model of Fe-Based Amorphous Magnet Materials. *J. Magn. Magn. Mater.* **2020**, *514*, 167290. [CrossRef]
65. Jensen, C.C.; Profumo, F.; Lipo, T.A. A Low-Loss Permanent-Magnet Brushless dc Motor Utilizing Tape Wound Amorphous Iron. *IEEE Trans. Ind. Appl.* **1992**, *28*, 646–651. [CrossRef]
66. Wang, Z.; Enomoto, Y.; Ito, M.; Masaki, R.; Morinaga, S.; Itabashi, H.; Tanigawa, S. Development of a Permanent Magnet Motor Utilizing Amorphous Wound Cores. *IEEE Trans. Magn.* **2010**, *46*, 570–573. [CrossRef]
67. Wang, L.; Li, J.; Li, S.; Zhang, G.; Huang, S. Development of the New Energy-Efficient Amorphous Iron Based Electric Motor. In Proceedings of the 2011 International Conference on Computer Distributed Control and Intelligent Environmental Monitoring, Changsha, China, 19–20 February 2011; pp. 2059–2061.
68. Fan, T.; Li, Q.; Wen, X. Development of a High Power Density Motor Made of Amorphous Alloy Cores. *IEEE Trans. Ind. Electron.* **2014**, *61*, 4510–4518. [CrossRef]
69. Tong, W.; Wu, S.; Sun, J.; Zhu, L. Iron Loss Analysis of Permanent Magnet Synchronous Motor with an Amorphous Stator Core. In Proceedings of the 2016 IEEE Vehicle Power and Propulsion Conference (VPPC), Hangzhou, China, 17–20 October 2016; pp. 1–6.
70. Tomioka, T.; Akatsu, K. Study of High-Speed SRM with Amorphous Steel Sheet for EV. In Proceedings of the 2016 19th International Conference on Electrical Machines and Systems (ICEMS), Chiba, Japan, 13–16 November 2016.
71. Li, T.; Zhang, Y.; Liang, Y.; Ai, Q.; Dou, H. Multiphysics Analysis of an Axial-Flux In-Wheel Motor With an Amorphous Alloy Stator. *IEEE Access* **2020**, *8*, 27414–27425. [CrossRef]

72. Fan, Z.; Yi, H.; Xu, J.; Xie, K.; Qi, Y.; Ren, S.; Wang, H. Performance Study and Optimization Design of High-Speed Amorphous Alloy Induction Motor. *Energies* **2021**, *14*, 2468. [CrossRef]

73. Persson, M.; Jansson, P.; Jack, A.G.; Mecrow, B.C. Soft Magnetic Composite Materials—Use for Electrical Machines. In Proceedings of the 1995 Seventh International Conference on Electrical Machines and Drives (Conf. Publ. No. 412), Durham, UK, 11–13 September 1995; pp. 242–246.

74. Guo, Y.; Zhu, J. Applications of Soft Magnetic Composite Materials in Electrical Machines: A Review. *Aust. J. Electr. Electron. Eng.* **2006**, *3*, 37–46. [CrossRef]

75. Ahmed, N.; Atkinson, G.J. A Review of Soft Magnetic Composite Materials and Applications. In Proceedings of the 2022 International Conference on Electrical Machines (ICEM), Valencia, Spain, 5–8 September 2022; pp. 551–557.

76. Guo, Y.; Ba, X.; Liu, L.; Lu, H.; Lei, G.; Yin, W.; Zhu, J. A Review of Electric Motors with Soft Magnetic Composite Cores for Electric Drives. *Energies* **2023**, *16*, 2053. [CrossRef]

77. Jack, A.G.; Mecrow, B.C.; Maddison, C.P. Combined Radial and Axial Magnet Motors Using Soft Magnetic Composites. In Proceedings of the 1999 Ninth International Conference on Electrical Machines and Drives (Conf. Publ. No. 468), Canterbury, UK, 1–3 September 1999; pp. 25–29.

78. Cvetkovski, G.; Petkovska, L.; Cundev, M.; Gair, S. Improved Design of a Novel PM Disk Motor by Using Soft Magnetic Composite Material. *IEEE Trans. Magn.* **2002**, *38*, 3165–3167. [CrossRef]

79. Kin, C.-W.; Jang, G.-H.; Kim, J.-M.; Ahn, J.-H.; Baek, C.-H.; Choi, J.-Y. Comparison of Axial Flux Permanent Magnet Synchronous Machines With Electrical Steel Core and Soft Magnetic Composite Core. *IEEE Trans. Magn.* **2017**, *53*, 8210004.

80. Aoyama, M.; Tsuya, H.; Hirata, S.; Sjoberg, L. Experience of Toroidally Wound Double Stator Axial-Gap Induction Machine With Soft Magnetic Composites. *IEEE Open J. Ind. Appl.* **2021**, *2*, 378–383. [CrossRef]

81. Qu, R.; Kliman, G.B.; Carl, R. Split-Phase Claw-Pole Induction Machines with Soft Magnetic Composite Cores. In Proceedings of the 39th IAS Annual Meeting, Seattle, WA, USA, 3–7 October 2004; pp. 2514–2519.

82. Guo, Y.; Zhu, J.G.; Watterson, P.A.; Wu, W. Development of a Permanent Magnet Claw Pole Motor with Soft Magnetic Composite Core. *Aust. J. Electr. Electron. Eng.* **2005**, *1*, 21–30. [CrossRef]

83. Guo, Y.G.; Zhu, J.G.; Ramsden, V.S. Design and Construction of a Single Phase Claw Pole Permanent Magnet Motor using Composite Magnetic Material. *Renew. Energy* **2001**, *22*, 185–195. [CrossRef]

84. Guo, Y.; Zhu, J.G.; Dorrell, D.G. Design and Analysis of a Claw Pole Permanent Magnet Motor with Molded SMC Core. *IEEE Trans. Magn.* **2009**, *45*, 4582–4585.

85. Liu, C.; Lu, J.; Wang, Y.; Lei, G.; Zhu, J.; Guo, Y. Design Issues for Claw Pole Machines with Soft Magnetic Composite Cores. *Energies* **2018**, *11*, 1998. [CrossRef]

86. Liu, C.; Liu, Q.; Wang, S.; Wang, Y.; Lei, G.; Guo, Y.; Zhu, J. A Novel Flux Switching Claw Pole Machine with Soft Magnetic Composite Cores. *Int. J. Appl. Electromagn. Mech.* **2021**, *67*, 183–203. [CrossRef]

87. Blissenbach, R.; Henneberger, G.; Schafer, U.; Hackmann, W. Development of a Transverse Flux Traction Motor in a Direct Drive System. In Proceedings of the IEEE Colloquium on New Topologies for Permanent Magnet Machines (Digest No: 1997/090), London, UK, 18 June 1997; pp. 1457–1460.

88. Guo, Y.; Zhu, J.G.; Watterson, P.A.; Wu, W. Development of a PM Transverse Flux Motor with Soft Magnetic Composite Core. *IEEE Trans. Energy Convers.* **2006**, *21*, 426–434. [CrossRef]

89. Zhu, J.G.; Guo, Y.G.; Lin, Z.W.; Li, Y.J.; Huang, Y.K. Development of PM Transverse Flux Motors with Soft Magnetic Composite Cores. *IEEE Trans. Magn.* **2011**, *47*, 4376–4383. [CrossRef]

90. Doering, J.; Steinborn, G.; Hofmann, W. Torque, Power, Losses, and Heat Calculation of a Transverse Flux Reluctance Machine with Soft Magnetic Composite Materials and Disk-Shaped Rotor. *IEEE Trans. Ind. Appl.* **2015**, *51*, 1494–1504. [CrossRef]

91. Liu, C.; Lei, G.; Ma, B.; Wang, Y.; Guo, Y.; Zhu, J. Development of a New Low-Cost 3-D Flux Transverse Flux FSPMM with Soft Magnetic Composite Cores and Ferrite Magnets. *IEEE Trans. Magn.* **2017**, *53*, 1–5. [CrossRef]

92. Rabenstein, L.; Dietz, A.; Parspour, N. Design Concept of a Wound Field Transverse Flux Machine Using Soft Magnetic Composite Claw-Poles. In Proceedings of the 2020 10th International Electric Drives Production Conference (EDPC), Ludwigsburg, Germany, 8–9 December 2020; pp. 1–5.

93. Zhang, F.; Du, G.; Wang, T.; Liu, G. Review on Development and Design of High Speed Machines. *Trans. China Electrotech. Soc.* **2016**, *31*, 1–18.

94. Maloberti, O.; Figueredo, R.; Marchand, C.; Choua, Y.; Condamin, D.; Kobylanski, L.; Bommé, E. 3-D–2-D Dynamic Magnetic Modeling of an Axial Flux Permanent Magnet Motor With Soft Magnetic Composites for Hybrid Electric Vehicles. *IEEE Trans. Magn.* **2014**, *50*, 1–11.

95. Kobler, R.; Andessner, D.; Weidenholzer, G.; Amrhein, W. Development of a Compact and Low Cost Axial Flux Machine Using Soft Magnetic Composite and Hard Ferrite. In Proceedings of the IEEE International Conference on Power Electronics and Drive Systems, Sydney, Australia, 9–12 June 2015; pp. 810–815.

96. Du, W.; Zhao, S.; Zhang, H.; Zhang, M.; Gao, J. A Novel Claw Pole Motor With Soft Magnetic Composites. *IEEE Trans. Magn.* **2021**, *57*, 8200904. [CrossRef]

97. Chu, S.; Liang, D.; Jia, S.; Liang, Y. Research and Analysis on Design Characteristics of High-Speed Permanent Magnet Claw Pole Motor With Soft Magnetic Composite Cores for Wide Temperature Range. *IEEE Trans. Ind. Appl.* **2022**, *58*, 7201–7213. [CrossRef]

98. Li, B.; Li, X.; Wang, S.; Liu, R.; Wang, Y.; Lin, Z. Analysis and Cogging Torque Minimization of a Novel Flux Reversal Claw Pole Machine with Soft Magnetic Composite Cores. *Energies* **2022**, *15*, 1285. [CrossRef]

99. Snitchler, G.; Gamble, B.; Kalsi, S.S. The Performance of a 5 MW High Temperature Superconductor Ship Propulsion Motor. *IEEE Trans. Appl. Supercond.* **2005**, *15*, 2206–2209. [CrossRef]

100. Gonzalez-Parada, A.; Espinosa-Loza, F.J.; Castaneda-Miranda, A.; Bosch-Tous, R.; Granados-Garcia, X. Application of HTS BSCCO Tapes in an Ironless Axial Flux Superconductor Motor. *IEEE Trans. Appl. Supercond.* **2012**, *22*, 5201004. [CrossRef]

101. Jin, J.X.; Zheng, L.H.; Guo, Y.G.; Grantham, C.; Sorrell, C.C.; Xu, W. High-Temperature Superconducting Linear Synchronous Motors Integrated With HTS Magnetic Levitation Components. *IEEE Trans. Appl. Supercond.* **2012**, *22*, 5202617.

102. Moon, H.; Kin, Y.-C.; Park, H.-J.; Park, M.; Yu, I.-K. Development of a MW-Class 2G HTS Ship Propulsion Motor. *IEEE Trans. Appl. Supercond.* **2016**, *26*, 5203805. [CrossRef]

103. Liu, B.; Badcock, R.; Shu, H.; Tan, L.; Fang, J. Electromagnetic Characteristic Analysis and Optimization Design of a Novel HTS Coreless Induction Motor For High-Speed Operation. *IEEE Trans. Appl. Supercond.* **2018**, *28*, 5202405. [CrossRef]

104. Zanegin, S.; Ivanov, N.; Zubko, V.; Kovalev, K.; Shishov, I.; Shishov, D.; Podguzov, V. Measurement and Analysis of AC Losses in HTS Windings of Electrical Machine for Different Operation Modes. *Appl. Sci.* **2021**, *11*, 2741. [CrossRef]

105. Brix, W.; Hempel, K.A.; Schulte, F.J. Improved Method for the Investigations of the Rotational Magnetization Process in Electrical Steel Sheets. *IEEE Trans. Magn.* **1984**, *20*, 1708–1710. [CrossRef]

106. Sievert, J. Recent Advances in the One- and Two-dimensional Magnetic Measurement Technique for Electrical Sheet Steel. *IEEE Trans. Magn.* **1990**, *26*, 2553–2558. [CrossRef]

107. Zhu, J.G.; Ramsden, V.S. Two Dimensional Measurement of Magnetic Field and Core Loss Using a Square Specimen Tester. *IEEE Trans. Magn.* **1993**, *29*, 2995–2997. [CrossRef]

108. Enokizono, M.; Tanabe, I. Studies on a New Simplified Rotational Loss Tester. *IEEE Trans. Magn.* **1997**, *33*, 4020–4022. [CrossRef]

109. Appino, C.; de la Barriere, O.; Beatrice, C.; Fiorillo, F.; Ragusa, C. Rotational Magnetic Losses in Nonoriented Fe-Si and Fe-Co Laminations up to the Kilohertz Range. *IEEE Trans. Magn.* **2014**, *50*, 2007104. [CrossRef]

110. Li, Y.; Cao, L.; Zhang, C.; Yang, Q.; Li, E. Rotational Core Loss of Silicon Steel Laminations Based on Three-Dimensional Magnetic Properties Measurement. *IEEE Trans. Appl. Supercond.* **2016**, *26*, 8201205. [CrossRef]

111. Akiror, J.C.; Wanjiku, J.; Pillay, P.; Cave, J.; Merkhouf, A. Rotational Core Loss Magnetizer: Design and Measurements. *IEEE Trans. Ind. Appl.* **2018**, *54*, 4355–4364. [CrossRef]

112. Zhong, J.J.; Zhu, J.G.; Ramsden, V.S.; Guo, Y. Magnetic Properties of Composite Soft Magnetic Materials with 2-D Fluxes. In Proceedings of the Australasian Universities Power Engineering Conference; University of Tasmania: Hobart, TAS, Australia, 1998; pp. 659–664.

113. Zhu, J.G.; Zhong, J.; Ramsden, V.S.; Guo, Y. Power Losses of Composite Soft Magnetic Materials under Two Dimensional Excitations. *J. Appl. Phys.* **1999**, *85*, 4403–4405. [CrossRef]

114. Guo, Y.; Zhu, J.G.; Zhong, J.J. Measurement and Modelling of Magnetic Properties of Soft Magnetic Composite Material under 2D Vector Magnetisations. *J. Magn. Magn. Mater.* **2006**, *312*, 14–19. [CrossRef]

115. Guo, Y.G.; Zhu, J.G.; Lin, Z.W.; Zhong, J.J. 3D Vector Magnetic Properties of Soft Magnetic Composite Material. *J. Magn. Magn. Mater.* **2006**, *302*, 511–516. [CrossRef]

116. Lin, Z.W.; Zhu, J.G.; Guo, Y.G. Three-Dimensional Hysteresis of Soft Magnetic Composite. *J. Appl. Phys.* **2006**, *99*, 08D909. [CrossRef]

117. Yang, Q.; Li, Y.; Zhao, Z.; Zhu, L.; Luo, Y.; Zhu, J. Design of a 3-D Rotational Magnetic Properties Measurement Structure for Soft Magnetic Materials. *IEEE Trans. Appl. Supercond.* **2014**, *24*, 8200804. [CrossRef]

118. Guo, Y.; Liu, L.; Ba, X.; Lu, H.; Lei, G.; Yin, W.; Zhu, J. Measurement and Modeling of Magnetic Materials under 3D Vectorial Magnetization for Electrical Machine Design and Analysis. *Energies* **2023**, *16*, 417. [CrossRef]

119. Sarker, P.C.; Guo, Y.; Lu, H.Y.; Zhu, J.G. Measurement and Modeling of Rotational Core Loss of Fe-Based Amorphous Magnetic Material under 2-D Magnetic Excitation. *IEEE Trans. Magn.* **2021**, *57*, 8402008. [CrossRef]

120. Guo, Y.; Liu, L.; Ba, X.; Lu, H.; Lei, G.; Yin, W.; Zhu, J. Characterization of Rotational Magnetic Properties of Amorphous Metal Materials for Advanced Electrical Machine Design and Analysis. *Energies* **2022**, *15*, 7798. [CrossRef]

121. Soomro, W.A.; Guo, Y.; Lu, H.; Jin, J.; Shen, B.; Zhu, J. Experimental Setup for Measurement of AC Loss in HTS under Rotating Magnetic Field. *Energies* **2022**, *15*, 7857. [CrossRef]

122. Soomro, W.A.; Guo, Y.; Lu, H.; Jin, J.; Shen, B.; Zhu, J. AC Loss in High-Temperature Superconducting Bulks Subjected to Alternating and Rotating Magnetic Field. *Materials* **2023**, *16*, 633. [CrossRef] [PubMed]

123. Enokizono, M.; Mori, S. A Treatment of the Magnetic Reluctivity Tensor for Rotating Magnetic Field. *IEEE Trans. Magn.* **1997**, *33*, 1608–1611. [CrossRef]

124. Guo, Y.; Zhu, J.G.; Lin, Z.W.; Zhong, J.J.; Lu, H.Y.; Wang, S. Determination of 3D Magnetic Reluctivity Tensor of Soft Magnetic Composite Material. *J. Magn. Magn. Mater.* **2007**, *312*, 458–463. [CrossRef]

125. Yoon, H.S.; Eum, Y.H.; Zhang, Y.; Shin, P.S.; Koh, C.S. Comparison of Magnetic Reluctivity Models for FEA Considering Two-Dimensional Magnetic Properties. *IEEE Trans. Magn.* **2009**, *45*, 1202–1205. [CrossRef]

126. Sun, J.; Yang, Q.; Wang, Y.; Yan, W.; Li, Y. A Finite Element Formulation for Tetrahedral Elements Based on Reluctivity Tensor. *IEEE Trans. Appl. Supercond.* **2010**, *20*, 1852–1855.

127. Li, Y.; Yang, Q.; Zhu, J.; Lin, Z.; Guo, Y.; Sun, J. Research of Three-Dimensional Magnetic Reluctivity Tensor Based on Measurement of Magnetic Properties. *IEEE Trans. Appl. Supercond.* **2010**, *20*, 1932–1935.
128. Padilha, J.B.; Kuo-Peng, P.; Sadowski, N.; Batistela, N.J. Vector Hysteresis Model Associated to FEM in a Hysteresis Motor Modeling. *IEEE Trans. Magn.* **2017**, *53*, 7402004. [CrossRef]
129. Guo, Y.G.; Zhu, J.G.; Lin, Z.W.; Zhong, J.J. Measurement and Modeling of Core Losses of Soft Magnetic Composites Under 3-D Magnetic Excitations in Rotating Motors. *IEEE Trans. Magn.* **2005**, *41*, 3925–3927.
130. Bertotti, G.; Boglietti, A.; Chiampi, M.; Chiarabaglio, D.; Fiorillo, F.; Lazzari, M. An Improved Estimation of Iron Losses in Rotating Machines. *IEEE Trans. Magn.* **1991**, *27*, 5007–5009. [CrossRef]
131. Zhu, J.G.; Ramsden, V.S. Improved Formulations for Rotational Core Losses in Rotating Electrical Machines. *IEEE Trans. Magn.* **1998**, *34*, 2234–2242.
132. Guo, Y.; Zhu, J.; Lu, H.; Lin, Z.; Li, Y. Core Loss Calculations for Soft Magnetic Composite Electrical Machines. *IEEE Trans. Magn.* **2012**, *48*, 3112–3115. [CrossRef]
133. Fiorillo, F.; Rietto, A.M. Rotational and Alternating Energy Loss versus Magnetizing Frequency in SiFe Laminations. *J. Magn. Magn. Mater.* **1993**, *83*, 402–404. [CrossRef]
134. Zhu, J.G.; Ramsden, V.S.; Sievert, J.D. Prediction of Core Loss with Elliptical Flux from Measurements with Alternating and Circular Fluxes in Electrical Steel Sheets. In Proceedings of the International ISEM Symposium on Advanced Computational and Design Techniques in Applied Electromagnetic Systems, Seoul, Republic of Korea, 22–24 June 1994; pp. 675–678.
135. Knorr, B.; Devarajan, D.; Lin, D.; Zhou, P.; Stanton, S. Application of Multi-level Multi-Domain Modeling to a Claw Pole Alternator. In Proceedings of the Annual Conference Society of Automotive Engineers, Salt Lake City, UT, USA, 20–23 June 2004.
136. Guo, Y.; Zhu, J.; Liu, D.; Lu, H.; Wang, S. Application of Multi-level Multi-domain Modeling in the Design and Analysis of a PM Transverse Flux Motor with SMC Core. In Proceedings of the 2007 7th International Conference on Power Electronics and Drive Systems, Bangkok, Thailand, 27–30 November 2007; pp. 27–31.
137. Wang, S.; Meng, X.; Guo, N.; Li, H.; Qiu, J.; Zhu, J.G.; Guo, Y.; Liu, D.; Wang, Y.; Xu, W. Multilevel Optimization for Surface Mounted PM Machines Incorporating With FEM. *IEEE Trans. Magn.* **2009**, *45*, 4700–4703. [CrossRef]
138. Lei, G.; Guo, Y.G.; Zhu, J.G.; Wang, T.S.; Chen, X.M.; Shao, K.R. System Level Six Sigma Robust Optimization of a Drive System With PM Transverse Flux Machine. *IEEE Trans. Magn.* **2012**, *48*, 923–926. [CrossRef]
139. Lei, G.; Wang, T.; Guo, Y.; Zhu, J.; Wang, S. System-Level Design Optimization Methods for Electrical Drive Systems: Deterministic Approach. *IEEE Trans. Ind. Electron.* **2014**, *61*, 6591–6602. [CrossRef]
140. Lei, G.; Wang, T.; Zhu, J.; Guo, Y.; Wang, S. System-Level Design Optimization Methods for Electrical Drive Systems-Robust Approach. *IEEE Trans. Ind. Electron.* **2015**, *62*, 4702–4713. [CrossRef]
141. Lei, G.; Liu, C.; Zhu, J.; Guo, Y. Techniques for Multilevel Design Optimization of Permanent Magnet Motors. *IEEE Trans. Energy Convers.* **2015**, *30*, 1574–1584. [CrossRef]
142. Asef, P.; Perpina, R.B.; Moazami, S.; Lapthorn, A.C. Rotor Shape Multi-Level Design Optimization for Double-Stator Permanent Magnet Synchronous Motors. *IEEE Trans. Energy Convers.* **2019**, *34*, 1223–1231. [CrossRef]
143. Meng, Y.; Fang, S.; Pan, Z.; Liu, W.; Qin, L. Machine Learning Techniques Based Multi-Level Optimization Design of a Dual-Stator Flux Modulated Machine With Dual-PM Excitation. *IEEE Trans. Transp. Electrif.* **2022**. *early access*. [CrossRef]
144. Zhu, X.; Shu, Z.; Quan, L.; Xiang, Z.; Pan, X. Multi-Objective Optimization of an Outer-Rotor V-Shaped Permanent Magnet Flux Switching Motor Based on Multi-Level Design Method. *IEEE Trans. Magn.* **2016**, *52*, 8205508. [CrossRef]
145. Lei, G.; Wang, T.; Zhu, J.; Guo, Y. Robust Multiobjective and Multidisciplinary Design Optimization of Electrical Drive System. *CES Trans. Electr. Mach. Syst.* **2018**, *2*, 409–416. [CrossRef]
146. Ma, Y.; Ching, T.W.; Fu, W.N.; Niu, S. Multi-Objective Optimization of a Direct-Drive Dual-Structure Permanent Magnet Machine. *IEEE Trans. Magn.* **2019**, *55*, 7501704. [CrossRef]
147. Diao, K.; Sun, X.; Lei, G.; Guo, Y.; Zhu, J. Multiobjective System Level Optimization Method for Switched Reluctance Motor Drive Systems Using Finite Element Model. *IEEE Trans. Ind. Electron.* **2020**, *67*, 10055–10064. [CrossRef]
148. Soltani, M.; Nuzzo, S.; Barater, D.; Franceschini, G. A Multi-Objective Design Optimization for a Permanent Magnet Synchronous Machine with Hairpin Winding Intended for Transport Applications. *Electronics* **2021**, *10*, 3162. [CrossRef]
149. Lei, G.; Liu, C.; Zhu, J.; Guo, Y. Multidisciplinary Design Analysis and Optimization of a PM Transverse Flux Machine with Soft Magnetic Composite Core. *IEEE Trans. Magn.* **2015**, *51*, 8109704. [CrossRef]
150. Popescu, M.; Foley, I.; Staton, D.A.; Goss, J.E. Multi-physics Analysis of a High Torque Density Motor for Electric Racing Cars. In Proceedings of the 2015 IEEE Energy Conversion Congress and Exposition (ECCE), Montreal, QC, Canada, 20–24 September 2015; pp. 6537–6544.
151. Lei, G.; Zhu, J.; Guo, Y. *Multidisciplinary Design Optimization Methods for Electrical Machines and Drive Systems*; Springer: Berlin/Heidelberg, Germany, 2016.
152. Dai, Z.; Wang, L.; Meng, L.; Yang, S.; Mao, L. Multi-Level Modeling Methodology for Optimal Design of Electric Machines Based on Multi-Disciplinary Design Optimization. *Energies* **2019**, *12*, 4173. [CrossRef]
153. Abdelrahman, A.; Sahu, A.; Emery, N.; Al-Ani, D.; Bilgin, B. Multi-physics Design Platform for a High Power Density Multi-phase IPM Traction Motor: Analysis and Simulation. In Proceedings of the 2022 IEEE Transportation Electrification Conference & Expo (ITEC), Anaheim, CA, USA, 15–17 June 2022; pp. 92–96.

154. Liu, G.; Liu, M.; Zhang, Y.; Wang, H.; Gerada, C. High-Speed Permanent Magnet Synchronous Motor Iron Loss Calculation Method Considering Multiphysics Factors. *IEEE Trans. Ind. Electron.* **2020**, *67*, 5360–5368. [CrossRef]
155. Li, D.; Zhang, Y.; Jing, Y.; Xie, D.; Koh, C.-S. Core Loss and Deformation Computation in Permanent Magnet Linear Motors Considering the Effect of Stress on Magnetic and Magnetostrictive Properties. In Proceedings of the 2021 13th International Symposium on Linear Drives for Industry Applications (LDIA), Wuhan, China, 1–3 July 2021; pp. 1–5.
156. Liu, L.; Ba, X.; Guo, Y.; Lei, G.; Sun, X.; Zhu, J. Improved Iron Loss Prediction Models for Interior PMSMs Considering Coupling Effects of Multiphysics Factors. *IEEE Trans. Transp. Electrif.* **2023**, *9*, 416–427. [CrossRef]
157. Gandzha, S.; Aminov, D.; Kiessh, I.; Kosimov, B. Application of Digital Twins Technology for Analysis of Brushless Electric Machines with Axial Magnetic Flux. In Proceedings of the 2018 Global Smart Industry Conference (GloSIC), Chelyabinsk, Russia, 13–15 November 2018; pp. 1–6.
158. Falekas, G.; Karlis, A. Digital Twin in Electrical Machine Control and Predictive Maintenance: State-of-the-Art and Future Prospects. *Energies* **2021**, *14*, 5933. [CrossRef]
159. Liu, L.; Guo, Y.; Yin, W.; Lei, G.; Zhu, J. Design and Optimization Technologies of Permanent Magnet Machines and Drive Systems Based on Digital Twin Model. *Energies* **2022**, *15*, 6186. [CrossRef]
160. Guo, Z.; Yan, S.; Xu, X.; Chen, Z.; Ren, Z. Twin-Model Based on Model Order Reduction for Rotating Motors. *IEEE Trans. Magn.* **2022**, *58*, 8206304. [CrossRef]